Thermal Conductivity and Thermoelectric Power of Yb-Substituted Bi-2212 Superconductor

H Gündoğmuş [1,2*], B Özçelik[2], A Sotelo[3] and M A Madre[3]

[1] Faculty of Engineering, Hakkari University, 30000 Hakkari, Turkey
[2] Department of Physics, Faculty of Sciences and Letters, Çukurova University. 01330 Adana, Turkey
[3] ICMA (CSIC-Universidad de Zaragoza) María de Luna, 3. 50018 Zaragoza, Spain

E-mail: hakangundogmus@hu.edu.tr

Abstract. In the present study, $Bi_2Sr_2CaCu_{2-x}Yb_xO_{8+y}$ where x = 0.0, 0.05, 0.1and 0.25, superconductor materials were textured using the Laser Floating Zone technique. After annealing the as-grown materials, they were characterized by thermal conductivity (κ-T), thermoelectric power (S-T), and electrical resistivity (R-T) measurements performed from room temperature down to 20 K. The thermoelectric power is positive in all cases and is found to increase with decreasing temperature, reaching the maximum value (peak) around the samples Tc values and dropping rapidly to zero below Tc. Electrical resistivity measurements show a slight decrease of T_C when Yb substitution is raised. In spite of this effect, T_C values are higher than 90 K in all cases. On the other hand, Yb substitution also decreases thermal conductivity, compared with the undoped samples.

1. Introduction

Since Bi-based superconductors $Bi_2Sr_2Ca_{n-1}Cu_nO_x$ (n = 1, 2, 3) were discovered by Maeda *et al*. [1] many substitutions have been made in BSCCO system in order to improve their physical and magnetic properties [2-14]. High-T_C Bi-based superconductor family is characterized by a high superconducting transition temperature $T_C \sim 90$ and 110 K for the phases with n = 2, and 3, respectively, and a high upper critical magnetic field, B_{c2}, which can reach 150 T [15]. The weak coupling between BiO-BiO layers in the BSCCO system enables substitution of rare-earth ions for Ca and/or Bi and makes the system interesting from the point of studying its structural, electrical, thermal and magnetic properties. It is well-known that the BSCCO system superconducting properties are very sensitive to the hole-carrier concentration which, in turn, depends on the substitution levels [16, 17].

In general, the studies of transport properties, such as electrical resistivity, thermoelectric power (S) and thermal conductivity (κ), are important for exploring the conduction mechanism and the nature of charge carriers. The thermoelectric properties of BSCCO have been investigated by many research groups [18-23]. It was reported that S values have been found to be positive, negative or both, depending on the substituting element and proportion. The presence of both positive and

negative values of the thermoelectric power indicates the effect of two types of charge carriers, i.e. holes and electrons, respectively. In addition, the material preparation techniques for the BSCCO systems play a crucial role. Laser Floating Zone Melting (LFZ) technique is one of the most reliable methods to texture these bulk superconductor samples [24]. This method provides well aligned Bi-2212 grains, with their c-axis nearly perpendicular to the growth direction, and very small amount of secondary phases. In previous works, the structural, physical, magneto resistance and superconducting properties of Yb-substituted BSCCO samples have been studied [6, 25]. In the present study, the electrical resistivity, thermoelectric power and thermal conductivity of LFZ textured $Bi_2Sr_2CaCu_{2-x}Yb_xO_{8+y}$ (x = 0.0, 0.05, 0.1, and 0.25) superconductors are presented. Moreover, with these data, the figure-of-merit, ZT ($=S^2T/\rho\kappa$) has been calculated to determine the thermoelectric performance of these samples.

2.Experimental Details

$Bi_2Sr_2CaCu_{2-x}Yb_xO_{8+y}$ samples, with x = 0.0, 0.05, 0.1, and 0.25, have been prepared by using a polymer matrix route described in detail in previous works [6]. In order to identify the present phases, powder X-ray diffraction patterns of the materials were recorded at room temperature using a Rigaku D/max-B powder diffract meter system working with CuK_α radiation and a constant scan rate between 2θ= 3-60º. Resistivity and thermal characterization measurements were carried out in a Quantum Design PPMS system. The $Bi_2Sr_2CaCu_{2-x}Yb_xO_{8+y}$ samples, with x = 0.0, 0.05, 0.1, and 0.25 will be hereafter named as A, B, C and D, respectively.

3.Results And Discussion

Normalized XRD diffraction patterns of A, B, C and D samples are displayed in Fig. 1. All samples mainly consist of Bi-2212 phase which indicates that the annealing process has been adequate. However, some impurity phases like $CaCuO_2$ were also detected. Unit cell parameters and particle sizes of samples are given table 1. As seen in Table 1, with increasing Yb content, a non-monotonic decrease of the c-parameter with simultaneous increase of the a-one was observed. Particle size calculations have been performed using Debye Scherer Formula [26].

$$L_{hkl}= 0{,}9\ \lambda / \beta\cos\theta \qquad (1)$$

where λ is the wavelength of the source, β is the full width at half maximum and θ is the angle. An indication of grain size can be roughly obtained from the peak width, if the diffraction peak is narrow, the crystal size is large. In Table 1, by using Eq.1, it can be seen that the particle sizes decrease with increasing Yb content.

Table 1. Unit cell parameters, particle size and hole-carrier concentration for the samples

Sample	**a=b (Å)**	**c(Å)**	**L_{hkl} (Å)**	***p***
A	3.834	30.950	371.1391	0.144
B	3.832	30.939	364.5567	0.138
C	3.832	30.900	332.2064	0.135
D	3.832	30.850	319.1931	0.135

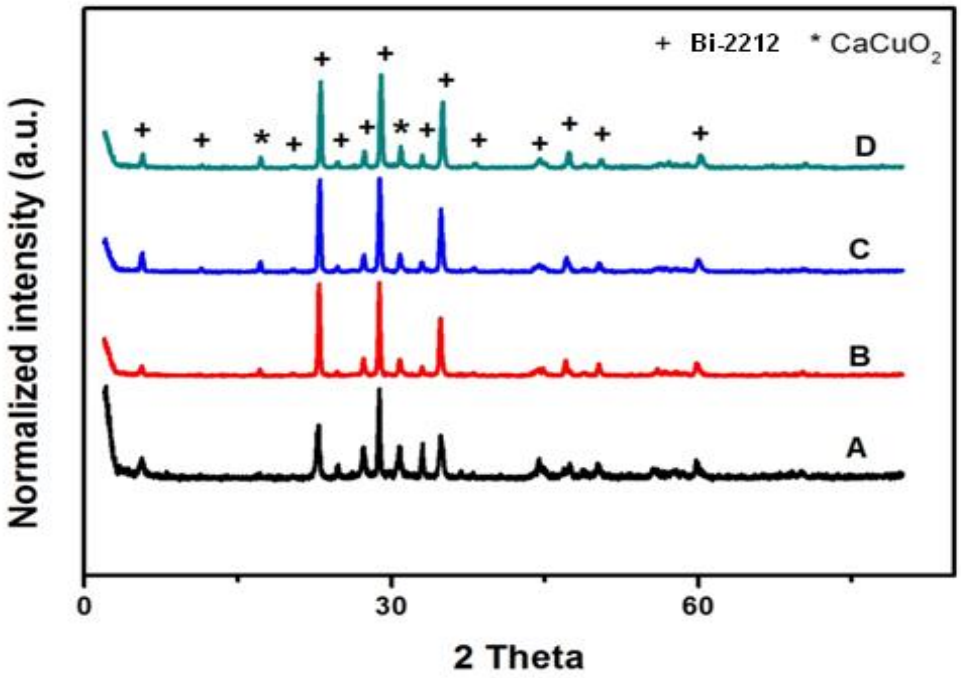

Figure 1. X-ray diffraction patterns of $Bi_2Sr_2CaCu_{2-x}Yb_xO_y$ superconducting samples

Fig. 2 shows the temperature dependence of the resistivity. The ρ curve shows a linear dependence with respect to the temperature between room and transition temperatures with metallic behavior. On the other hand, it can be clearly seen that T_c is approximately the same for all the samples. It is valuable to say that the increase of the resistivity in metallic region is due to the decrease of the grain alignment and the modification of grain size together with the appearance of secondary phases, as can be seen at XRD patterns. T_c^{onset} and T_c^{offset} temperatures are found as 100, 98.6, 97.7, and 96 K, and 95, 93.2, 92.1, and 90 K, for A, B, C and D samples, respectively. As a consequence, it is clear that Yb decreases T_C values but in a small extent. The temperature dependence of S for all the samples is given in Fig.3. All the samples exhibit positive S values indicating hole like conduction.

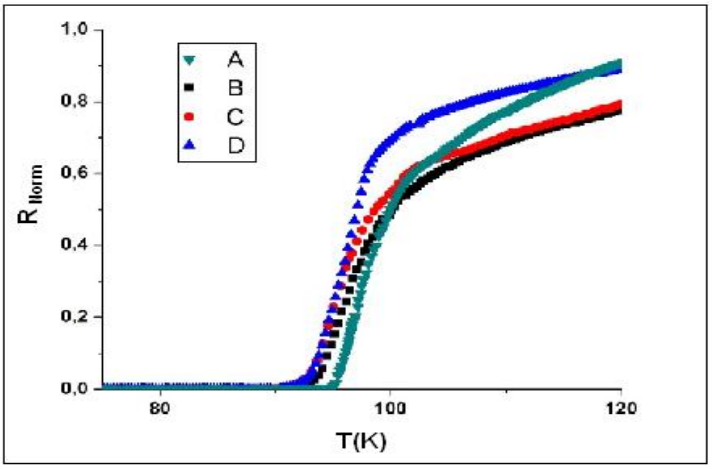

Figure 2. Temperature dependence of normalized resistivity for all the samples

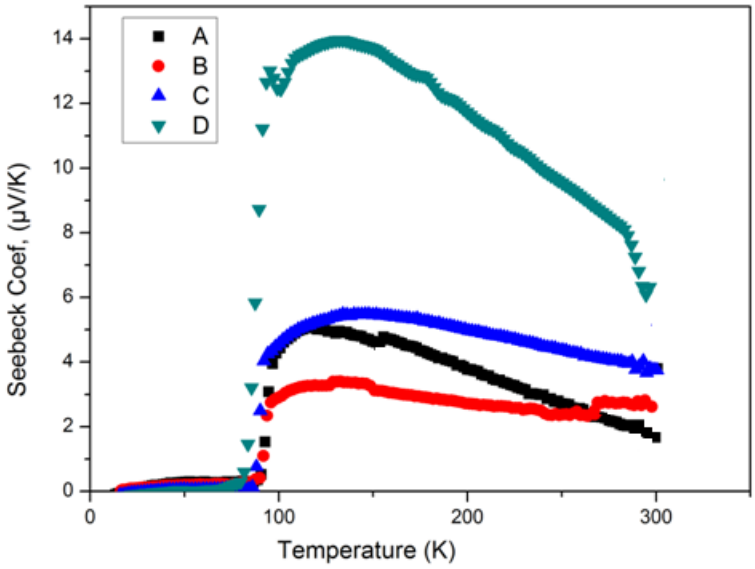

Figure 3. Temperature dependence of thermoelectric power for all the samples

This is similar to those observed for the substituted BSCCO system reported in other works [23, 27]. The positive *S*-values obtained in these samples are caused by the contribution of Bi-2212 phase. Furthermore, *S* increases by decreasing the temperature, and attain maximum values at around their respective transition temperature values, before dropping to zero at lower ones, as expected. Moreover, in spite of the anomalous behavior of B sample, as a general trend it can be deduced that the magnitude of *S* increases with Yb-content.

In Fig. 4, the temperature dependence of thermal conductivity for all the samples is exhibited. As can be observed, for $T>Tc$ (metallic state), κ first linearly increases from room temperature, reaching a maximum and then decreases with decreasing temperature. Around *Tc*, first a shallow minimum was observed following by a small raise. Then with decreasing *T*, almost a linear decrease towards zero was found.

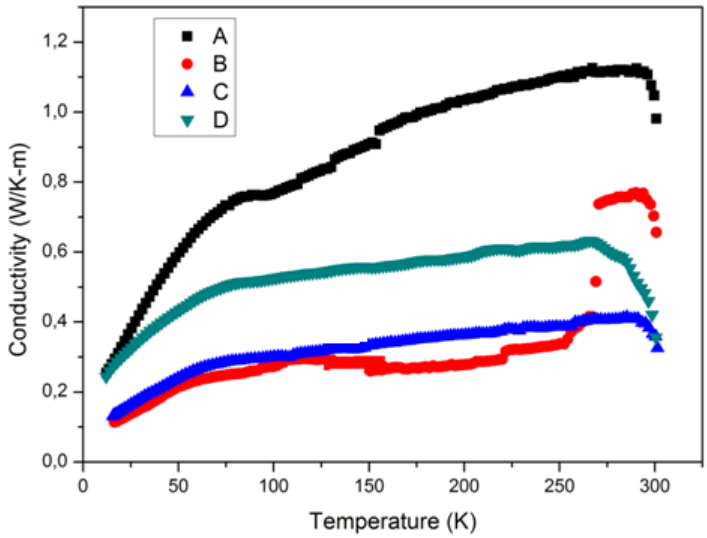

Figure 4. Temperature dependence of the thermal conductivity for all the samples

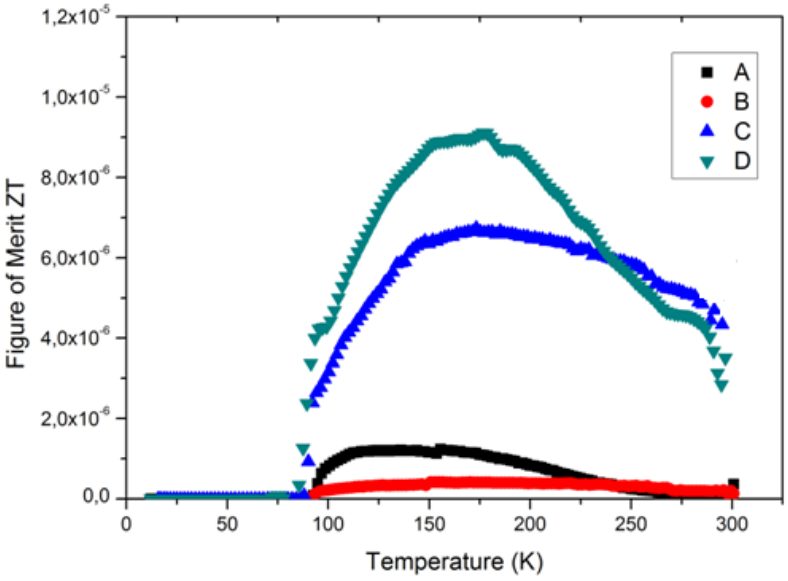

Figure 5. Figure of Merit for the samples

This type of behavior has previously been reported in the H*Tc* systems [22, 23, 28, 29]. The origin of the minimum can be attributed to the superconducting fluctuations [30, 31]. These results reveal that the magnitude of the thermal conductivity, κ, is influenced by the Yb- concentration in the system. Namely, with increasing Yb concentration the magnitude of κ is decreased. The dimensionless figure of merit, ZT, is defined as:

$$ZT = \alpha^2 T/\rho\kappa \qquad (2)$$

where T, α, ρ, κ are temperature, thermoelectric power, electrical resistivity and thermal conductivity, respectively. According to Eq.2, ZT is maximized when the thermoelectric power increases and the electrical resistivity and thermal conductivity decrease. As can be seen in Fig. 5, ZT is maximized at the temperature where thermoelectric power is maximized. Moreover, it becomes zero below the transition temperature of each compound. Furthermore, it is clear that the general trend is increasing ZT with Yb content.

4.Conclusions

Textured $Bi_2Sr_2CaCu_{2-x}Yb_xO_y$ superconducting materials with x= 0.0, 0.05, 0.1, and 0.25 were successfully prepared by the LFZ technique. Electrical resistivity measurements show that Yb substitution slightly decreases T_c. Nevertheless, the minimum measured value is still higher than 90 K. Thermoelectric power is increasing with Yb content while thermal conductivity is decreased. All these factors lead to an important raise of ZT for the Yb-doped materials which is maximum for the 0.25Yb-doped samples. Moreover, the improvement of ZT is about 5 times the measured in undoped samples.

Acknowledgements

This work is supported by Research Fund of Çukurova University, Adana, Turkey, under grant contracts no: FEF 2011D21.

References

[1] Maeda H *et al*. 1988 *Jpn*. *J*. *Appl*. *Phys*. **27** L 209
[2] Özçelik B *et al*. *Mater*. *Sci: Mater Electron*. **25** 2456
[3] Özçelik B *et al*. 2014 *J*. *Low Temp*. *Phys*. **174** 136
[4] Türk N *et al*. 2014 *J Supercond*. *Nov*. *Magn*. **27** 711
[5] Özaslan A *et al*. 2014 *J*. *Supercond*. *Nov*. *Magn*. **27** 53
[6] Gündogmus H *et al*. *2013 J*. *Supercond*. *Nov*. *Magn*, **26** 111
[7] Ozcelik B *et al*. 2014 J. *Mater*. *Sci: Mater Electron*. **25** 4476
[8] Özçelik B *et al*. 2013 *J*. *Supercond*. *Nov*. *Magn*. **26** 873
[9] Yazıcı D *et al*. 2011 *J*. *Low Temp*. *Phys*. **163** 370
[10] Özkurt B *et al*. 2012 J. *Supercond*. *Nov*. *Mag*. **25** 799
[11] Ozcelik B *et al*. 2015 *J*. *Supercond*. *Nov*. *Magn*. **28** 553
[12] Ozcelik B *et al*. 2015 *J*. *Mater*. *Sci: Mater Electron*. **26** 441
[13] Ozcelik B *et al*. 2015 *J*. *Mater*. *Sci: Mater Electron DOI* **10.**1007/s10854-015-2765-1
[14] Gursul M *et al*. 2015 *J*. *Supercond*. *Nov*. *Magn*. DOI **10**.1007/s10948-015-2977-x
[15] Blatter G *et al*. 1994 *Rev*. *Mod*.*Phys*. **6 1**125
[16] Torrance J B *et al*. 1998 *Phys*.*Rev*. *Lett*. **61** 1127
[17] Tokura Y *et al*. 1998 *Phys*. *Rev*. B **38** 7156
[18] Chatterjee S *et al*. 1996 *Phys*. *Rev*. B **53** 5942
[19] Yakinci M E *et al*. 2007 *Physica C **460*** 1386
[20] Bhattacharya S 1998 *J*. *Mater*. *Sci*. *Lett*. **17** 1575
[21] Aksan M A *et al*. 2004 *J*. *Alloy Comp*. ***385*** 33
[22] Ozkurt B *et al*. 2007 *Physica C*. **467** 112
[23] Ozkurt B *et al*. 2007 *Low Temp*.*Phys*. **147** No:1/2 April 31
[24] De la Fuente G F *et al*. 1995 *Adv*. *Mater*. **7** 853
[25] Yakinci M E 1997 *J*. *of Phy*. *Con*. *Matt*. **9** 1105
[26] Cullity B D 1978 *Element of X-ray Differaction, Addition-Wesley, Reading, MA*
[27] Kishore K N *et al*. 1995 *Physica C*. **252** 49
[28] Chanda B *et al* 1994 *Solid State Commun*. **89** 353
[29] Aksan M A *et al*. 1999 *J*. *Low Temp*. *Phys*. **117** 957
[30] Cohn J L *et al*. 1992 *Phys*. *Rev*. **B 45** 13144
[31] Castellazi S *et al*. 1997 *Physica C*. **273** 314